

# Current-voltage characteristics of the two-dimensional $XY$ model with Monte Carlo dynamics

Beom Jun Kim

*Department of Theoretical Physics, Umeå University, 901 87 Umeå, Sweden*

Current-voltage characteristics and the linear resistance of the two-dimensional  $XY$  model with and without external uniform current driving are studied by Monte Carlo simulations. We apply the standard finite-size scaling analysis to get the dynamic critical exponent  $z$  at various temperatures. From the comparison with the resistively-shunted junction dynamics, it is concluded that  $z$  is universal in the sense that it does not depend on details of dynamics. This comparison also leads to the quantification of the time in the Monte Carlo dynamic simulation.

PACS numbers: 75.40.Gb, 74.50.+r, 74.25.Fy, 64.60.Ht

Equilibrium properties of the two-dimensional (2D)  $XY$  model have been studied extensively and there are well-established consensus on them.<sup>1</sup> Dynamic properties of 2D  $XY$  model, however, are still under strong debate: For example, some studies on the dynamic critical exponent  $z$  seem to contradict each other.<sup>2-8</sup> Investigation of dynamic properties requires a set of dynamic equations or impositions of update rules and there exist various possible choices for the  $XY$  model. On the one hand, there are Langevin-type stochastic equations like the resistively shunted junction (RSJ) dynamics for  $XY$  model with phase representation,<sup>2,3,6</sup> and the relaxational dynamics (often called the time-dependent Ginzburg Landau dynamics) for both phase<sup>2,3,9</sup> and vortex representations.<sup>7</sup> On the other hand, it is also possible to use Monte Carlo (MC) simulations to study dynamic behaviors<sup>8,10</sup> although the identification of a Monte Carlo update step with a time step still lacks a complete rigorous justification.<sup>11</sup> An understanding of the dynamic transport properties, like the current-voltage characteristics, in the above dynamic models are important also in the practical sense, since such properties are directly measured in experiments on  $XY$ -like realizations such as Josephson-junction arrays and high- $T_c$  superconductors.

We here use the standard MC simulation method to study the current-voltage characteristics of the  $XY$  model with phase representation. The purpose of the current investigation is to find the dynamic critical exponent  $z$  in MC dynamic simulation and compare it with existing results from other dynamics. It then turns out that it is possible to quantify the MC time scales from the comparison with RSJ dynamics (see Ref. 12 for a recent discussion on the time quantification of MC dynamics). This opens a possibility to use MC simulation, which is usually much more efficient than direct numerical integrations of stochastic equations of motion, to examine many interesting long-time dynamic properties of the  $XY$  models.

The fluctuating twist boundary condition (FTBC) has been introduced first in the static MC simulation,<sup>13</sup> and later has been extended to RSJ dynamics.<sup>2</sup> In the computations of dynamic quantities, it has been shown that the

FTBC has some advantage over the periodic boundary condition: For example, the fluctuating linear resistance can be calculated in a much more convenient way in the FTBC.<sup>2,3</sup> We start from the RSJ dynamic equations of motion for the 2D  $XY$  model on a square lattice in the presence of an external current in the  $x$  direction with the current density  $\mathbf{J} = (J, 0)$  under the FTBC.<sup>2</sup> The phase variable  $\theta_i$  on the  $i$ th site at position  $\mathbf{r}_i$  satisfies<sup>14</sup>

$$\begin{aligned}\dot{\theta}_i &= - \sum_j G_{ij} \sum_k' [\sin(\theta_j - \theta_k - \Delta \cdot \mathbf{r}_{jk}) + \eta_{jk}] \\ &\equiv h_i - \sum_j G_{ij} \sum_k' \eta_{jk},\end{aligned}\quad (1)$$

where  $G_{ij}$  is the lattice Green function, the primed summation is over nearest-neighbor sites ( $k$ ) of  $j$ ,  $\Delta = (\Delta_x, \Delta_y)$  is the fluctuating twist variable, and  $\mathbf{r}_{jk} \equiv \mathbf{r}_k - \mathbf{r}_j$ . The thermal noise  $\eta_{ij}$  is white noise satisfying  $\langle \eta_{ij} \rangle = 0$  and  $\langle \eta_{ij}(t) \eta_{kl}(0) \rangle = 2T(\delta_{ik}\delta_{jl} - \delta_{il}\delta_{jk})\delta(t)$ , with the temperature  $T$  in units of Josephson coupling strength. The equations of motion for  $\Delta$  are written as

$$\begin{aligned}\frac{d\Delta_x}{dt} &= \frac{1}{L^2} \sum_{\langle ij \rangle_x} \sin(\theta_i - \theta_j - \Delta_x) + \eta_{\Delta_x} - J \\ &\equiv h_x + \eta_{\Delta_x} - J,\end{aligned}\quad (2)$$

$$\begin{aligned}\frac{d\Delta_y}{dt} &= \frac{1}{L^2} \sum_{\langle ij \rangle_y} \sin(\theta_i - \theta_j - \Delta_y) + \eta_{\Delta_y} \\ &\equiv h_y + \eta_{\Delta_y},\end{aligned}\quad (3)$$

where  $\sum_{\langle ij \rangle_x}$  denotes the summation over all links in the  $x$  direction, and the thermal noise terms satisfy  $\langle \eta_{\Delta_x} \rangle = \langle \eta_{\Delta_y} \rangle = \langle \eta_{\Delta_x} \eta_{\Delta_y} \rangle = 0$  and  $\langle \eta_{\Delta_x}(t) \eta_{\Delta_x}(0) \rangle = \langle \eta_{\Delta_y}(t) \eta_{\Delta_y}(0) \rangle = (2T/L^2)\delta(t)$ . The above Langevin-type equations of motion (1)-(3) can be cast into the Fokker-Planck equation for the probability distribution function  $P$ :

$$\begin{aligned}\frac{\partial P}{\partial t} &= - \sum_i \frac{\partial}{\partial \theta_i} h_i P - \frac{\partial}{\partial \Delta_x} h_x P - \frac{\partial}{\partial \Delta_y} h_y P \\ &\quad + T \sum_{ij} G_{ij} \frac{\partial^2 P}{\partial \theta_i \partial \theta_j} + \frac{T}{L^2} \left( \frac{\partial^2 P}{\partial \Delta_x^2} + \frac{\partial^2 P}{\partial \Delta_y^2} \right),\end{aligned}\quad (4)$$

whose stationary solution ( $\partial P/\partial t = 0$ ) in the form  $P = e^{-H/T}$  consequently leads to the effective Hamiltonian:<sup>15</sup>

$$H = - \sum_{\langle ij \rangle} \cos(\theta_i - \theta_j - \mathbf{\Delta} \cdot \mathbf{r}_{ij}) + L^2 \mathbf{J} \cdot \mathbf{\Delta}, \quad (5)$$

where the summation runs over all the nearest-neighbor bonds constituting the array. The Hamiltonian (5) is not invariant under the transformation  $\Delta_x \rightarrow \Delta_x + 2\pi$ , in contrast to the original RSJ equations. However, we note that in MC simulations the energy difference of configurations, not the energy itself, determines the time evolution of the system. Thus a direct use of Eq. (5) in the MC simulations does not cause any problem.

In the MC simulations, we first pick one site and try to rotate the phase angle at this site by an amount randomly chosen in  $[-\delta\theta, \delta\theta]$  (we call  $\delta\theta$  the trial angle range). This MC try is accepted according to the standard Metropolis algorithm applied to the Hamiltonian (5). After sweeping through all the lattice sites to update all the phase variables, we update the fluctuating twist variables  $\Delta_x$  and  $\Delta_y$  in a similar way: we try to rotate  $L\Delta_x$  and  $L\Delta_y$  within the angle range  $\delta\Delta$ . (For convenience, we use  $\delta\theta = \delta\Delta$ .) This complete update of the phase variables and the twist variables constitute one MC step. It is this MC step which is identified with one time step. A static quantity in equilibrium does not depend on the choice of  $\delta\theta$ ; the choice of  $\delta\theta$  only affects the convergence rate of the quantity (too small and too large  $\delta\theta$  worsen the convergence). This is contrary to a dynamic quantity which in general is expected to depend on  $\delta\theta$ . In Ref. 12, from the study of the anisotropic magnetic particle in an external magnetic field, it has been shown that as far as long-time behaviors are concerned the real dynamics and MC dynamics become in good agreements when the time evolution in MC simulation becomes slow enough. If such a result also did carry over to our model it would for our MC simulation imply that the MC dynamics give the same current-voltage characteristics as the RSJ dynamics after a suitable normalization of time, when  $\delta\theta$  is sufficiently small. As will be shown below, we find that this is indeed the case.

In the absence of external current [ $\mathbf{J} = 0$  in Eq. (5)], we first calculate  $L\Delta_x$  as a function of time, typically up to  $t = 10^9$ - $10^{10}$  after equilibration, and then compute the fluctuating linear resistance<sup>2</sup>

$$R_{\text{lin}} = \frac{1}{2T} \frac{1}{\Theta} \langle [L\Delta_x(\Theta) - L\Delta_x(0)]^2 \rangle, \quad (6)$$

where  $\Theta$  is chosen to be sufficiently large and  $\langle \dots \rangle$  is substituted by the time average (see Refs. 3 and 16). The linear resistance is closely related with the time scale  $\tau$ , defined by the time spent between the jumps of  $L\Delta_x$  by  $2\pi$  (see Fig. 8 in Ref. 2).

$$R_{\text{lin}} = \frac{1}{2T} \frac{(2\pi)^2}{\tau}. \quad (7)$$

In other words, the linear resistance is obtained from the equilibrium fluctuations of  $L\Delta_x$  which has a time scale  $\tau$  related with jumps by  $2\pi$ . Since the computation of  $R_{\text{lin}}$  in practice is more straightforward than  $\tau$ , we calculate the former and  $\tau$  is simply obtained by Eq. (6).<sup>17</sup> As is well known, the whole low-temperature phase of the 2D *XY* model is quasi-critical and the dynamic critical exponent  $z$  is defined by  $\tau \sim L^z$  due to the infinite correlation length. Alternatively,  $z$  can be computed from Eq. (7)

$$R_{\text{lin}} \sim L^{-z} \quad (8)$$

at a given temperature  $T$ . Although there exist several studies with a different conclusion,<sup>18</sup> there is nevertheless a growing consensus that the 2D *XY* model in the low-temperature phase has a  $z$  which is a monotonically decreasing function of  $T$ . Figure 1 displays (a)  $R_{\text{lin}}$  vs  $L$  at various  $T$  and (b)  $R_{\text{lin}}$  vs  $T$  for various  $L$ , for the trial angle range  $\delta\theta = \pi/6$ . As expected, the dynamic critical exponent  $z$  defined by Eq. (8) becomes larger as  $T$  is lowered. The dependence of  $R_{\text{lin}}$  on  $\delta\theta$  is also studied: we find that although the value of  $R_{\text{lin}}$  strongly depends on  $\delta\theta$ , the exponent  $z$  appears to saturate as  $\delta\theta$  is decreased, as shown in Fig. 2, where  $z(\delta\theta = \pi/18) \approx z(\pi/6)$  (the bigger deviations at lower temperatures are due to the poor convergences in  $R_{\text{lin}}$  at  $\delta\theta = \pi/18$  since very long time evolution is needed due to very large characteristic time). Since the time scale is inversely proportional to the linear resistance [see Eq. (7)], Fig. 2 implies that the time scales at  $\delta\theta = \pi/6$  and  $\pi/18$  are simply proportional to each other in a broad range of temperatures and system sizes; we numerically find  $\tau(T, L, \delta\theta = \pi/6) \approx c\tau(T, L, \delta\theta = \pi/18)$  with  $c \approx 0.14$  independent of  $T$  and  $L$ .

If driven by an external current in the  $x$  direction, the twist variable  $\Delta_x$  decreases as time goes on since the smaller  $\Delta_x$  gives the lower energy [see Eq. (5)], and the system develops a voltage drop across the sample with the electric field

$$E = -\langle \dot{\Delta}_x \rangle. \quad (9)$$

We perform simulations for  $L = 4, 6, 8$ , and  $10$  at  $0.65 \leq T \leq 1.5$  with  $\delta\theta = \pi/6$  and  $\pi/18$ : Figure 3, as an example, displays the current-voltage characteristics ( $E$  vs  $J$ ) at various temperatures for  $L = 8$  and  $\delta\theta = \pi/6$ . At low currents, the current-voltage characteristics become linear ( $E \sim J$ ) at any temperatures in accordance with Ref. 19 for RSJ dynamics.

In the low-temperature phase of the 2D *XY* model, the dynamic scaling in Ref. 20 for the current-voltage characteristics takes the form<sup>2,19</sup>

$$E/J = L^{-z} f(JL), \quad (10)$$

where  $z$  and the scaling function  $f(x)$  depend on  $T$ . In Fig. 4, the finite-size scaling is exhibited in the form

$(E/J)L^z = f(JL)$  at  $T = 0.80$  for  $\delta\theta = \pi/6$ . In this construction  $z$  is the only one free parameter and  $z = 3.5(1)$  is obtained. The solid line in Fig. 4 is obtained from  $R_{\text{lin}}$  computed above in the absence of external currents.

Table I summarizes our MC results for  $z$  with and without external currents, i.e.,  $z$  from  $R_{\text{lin}}$  without current driving in Fig. 2, and  $z$  from the finite-size scaling of the current-voltage characteristics in the presence of external current (see Fig. 4). As seen from the table, these two different determinations are in agreement. In Table I we have also included the  $z$  values obtained for the RSJ dynamics in Ref. 2, and again find agreement. From this we conclude that the  $z$  values from the Monte Carlo dynamic simulation in the present work agree with the corresponding values from the RSJ dynamics.

The above agreements suggest that some features of the real time dynamics for the XY model can be studied by MC simulations. The practical advantage is that MC simulations are usually much more efficient than numerical integrations of stochastic dynamic equations like RSJ equations. In Fig. 5 we carry the comparison one step further: we directly compare the current-voltage characteristics obtained in this paper from MC at  $\delta\theta = \pi/6$  with that in Ref. 19 from RSJ, for  $L = 8$  at  $T = 0.90, 0.85,$  and  $0.80$  (from top to bottom). It is shown that multiplications of  $E$  from MC by factors 11.6, 10.9, and 10.1 for  $T = 0.90, 0.85,$  and  $0.80,$  respectively, result in perfect agreements within a broad range of  $J$  (the temperature-dependence of the conversion factor has also been found in Ref. 12). Since the resistance is inversely proportional to the time scale [see Eq. (7)], Fig. 5 leads to the result that the time scale of the MC simulation at  $\delta\theta = \pi/6$  for a given temperature is larger than RSJ dynamic simulation by the above constant factor.

In summary, we have performed the MC dynamic simulation of the 2D XY model subject to the fluctuating twist boundary condition with and without external currents. Through the use of the standard finite-size scaling method, the dynamic critical exponent  $z$  has been obtained as a function of temperature, and found to be in accordance with RSJ dynamic results in Ref. 2, as well as with the scaling prediction by Minnhagen *et al.* in Ref. 21. It has also been shown that the current-voltage characteristics obtained from MC dynamic simulation is in a good agreement with that from the RSJ dynamics, leading to the quantification of time in MC simulation.<sup>22</sup> This implies that it is possible to use MC dynamic simulation, which is much more efficient than numerical integration of stochastic dynamic equations in many cases, to study long-time behaviors of the real dynamics of the XY model. For example, the time-quantified MC simulation can be useful to study glass-like dynamic behaviors of the XY models with disorder,<sup>23</sup> as well as to investigate current-voltage characteristics of the XY model in very low temperatures where RSJ simulation takes too much time to get converged results.<sup>24</sup>

The author is grateful to Petter Minnhagen for useful discussions. This work was supported by the Swedish

Natural Research Council through Contract No. FU 04040-332.

- 
- <sup>1</sup> See for reviews, P. Minnhagen, Rev. Mod. Phys. **59**, 1001 (1987); *Proceedings of the 2nd CTP workshop on Statistical Physics: KT Transition and Superconducting Arrays*, edited by D. Kim, J. S. Chung, and M. Y. Choi (Min-Eum Sa, Seoul, 1996), and references therein.
  - <sup>2</sup> B. J. Kim, P. Minnhagen, and P. Olsson, Phys. Rev. B **59**, 11506 (1999).
  - <sup>3</sup> L. M. Jensen, B. J. Kim, and P. Minnhagen, Europhys. Lett. **49**, 644 (2000); Phys. Rev. B **61**, 15412 (2000).
  - <sup>4</sup> H. J. Luo and B. Zheng, Mod. Phys. Lett. B **11**, 615 (1997); A. J. Bray, A. J. Briant, and D. K. Jervis, Phys. Rev. Lett. **84**, 1503 (2000).
  - <sup>5</sup> S. M. Ammirata, M. Friesen, S. W. Pierson, L. A. Gorham, J. C. Hunnicutt, M. L. Trawick, C. D. Keener, Physica C **313**, 225 (1999); S. W. Pierson, M. Friesen, S. M. Ammirata, J. C. Hunnicutt, and L. A. Gorham, Phys. Rev. B **60**, 1309 (1999); S. W. Pierson and M. Friesen, Physica B **284**, 610 (2000).
  - <sup>6</sup> M. V. Simkin and J. M. Kosterlitz, Phys. Rev. B **55**, 11646 (1997).
  - <sup>7</sup> K. Holmlund and P. Minnhagen, Phys. Rev. B **54**, 523 (1996); Physica C **292**, 255 (1997).
  - <sup>8</sup> H. Weber, M. Wallin, and H. Jensen, Phys. Rev. B **53**, 8566 (1996).
  - <sup>9</sup> A. Jonsson and P. Minnhagen, Phys. Rev. B **55**, 9035 (1997).
  - <sup>10</sup> J.-R. Lee and S. Teitel, Phys. Rev. B **50**, 3149 (1994).
  - <sup>11</sup> M. Y. Choi and B. A. Huberman, Phys. Rev. B **28**, 2547 (1983); **29** 2796 (1984).
  - <sup>12</sup> U. Nowak, R. W. Chantrell, and E. C. Kennedy, Phys. Rev. Lett. **84**, 163 (2000); R. Smimov-Rueda, O. Chubykalo, U. Nowak, R. W. Chantrell, and J. M. Gonzalez, J. Appl. Phys. **87**, 4798 (2000).
  - <sup>13</sup> P. Olsson, Phys. Rev. B **46**, 14598 (1992); **52**, 4511 (1995); **52**, 4526 (1995).
  - <sup>14</sup> In RSJ model, we measure the time, the current, the energy, and the temperature in units of  $\hbar/2eRI_c$ ,  $I_c$ ,  $\hbar I_c/2e$ , and  $\hbar I_c/2ek_B$ , respectively ( $I_c$  is the single junction critical current and  $R$  is the shunt resistance).
  - <sup>15</sup> Alternatively, Eq. (5) also can be obtained from the effective Hamiltonian for the free boundary condition in the presence of an external current [see M. Y. Choi, Phys. Rev. B **46**, 564 (1992)] through a simple change of variables (see Ref. 2) and then imposing the periodicity,  $\theta_{i+L\hat{x}} = \theta_{i+L\hat{y}} = \theta_i$ .
  - <sup>16</sup> B. J. Kim, Phys. Rev. B **62**, 644 (2000).
  - <sup>17</sup> Equation (7) was verified numerically when the system size was small in this work. We also confirmed it from data presented in Ref. 2 for the resistively-shunted junction dynamics.
  - <sup>18</sup> The short-time relaxation method [see Z. B. Li, L. Schülke, and B. Zheng, Phys. Rev. Lett. **74**, 3396 (1995)] applied

for 2D  $XY$  model with Monte Carlo dynamic simulation has found  $z \approx 2$  in the whole low-temperature phase [see, e.g., Ref. 4], while the scaling method by Pierson *et al.* for various experiments and simulations has lead to a relatively large but temperature-independent value  $z \approx 6$  [Ref. 5].

<sup>19</sup> K. Medvedyeva, B. J. Kim, and P. Minnhagen, Phys. Rev. B (in press).

<sup>20</sup> D. S. Fisher, M. P. A. Fisher, and D. A. Huse, Phys. Rev. B **43**, 130 (1991).

<sup>21</sup> P. Minnhagen, O. Westman, A. Jonsson, and P. Olsson, Phys. Rev. Lett. **74**, 3672 (1995).

<sup>22</sup> With material parameters  $I_c = 7\text{mA}$  and the shunt resistance  $R = 2\text{m}\Omega$ , one MC step in this paper is found to approximately corresponds to  $10^{-10}$  sec.

<sup>23</sup> S. J. Lee (private communication).

<sup>24</sup> K. Medvedyeva, B. J. Kim, and P. Minnhagen, unpublished.

TABLE I. Dynamic critical exponent  $z$  of 2D  $XY$  model subject to Monte Carlo dynamics.  $z(R_{\text{lin}})$  is from the scaling of the linear resistance at  $\delta\theta = \pi/6$  (Fig. 2) and  $z(E-J)$  is from the finite-size scaling of the current-voltage characteristics (see Fig. 4). The results from the RSJ dynamics in Ref. 2 are also presented for comparisons.

$T$	0.65	0.70	0.75	0.80	0.85	0.90
$z(R_{\text{lin}})$	6.0(2)	5.2(1)	4.3(1)	3.5(1)	2.8(1)	2.2(1)
$z(E-J)$	5.9(3)	5.0(2)	4.3(2)	3.5(1)	2.8(1)	2.2(1)
$z(\text{RSJ})^{\text{a}}$	-	-	-	3.3(1)	2.7(1)	2.0(1)

<sup>a</sup> Reference 2

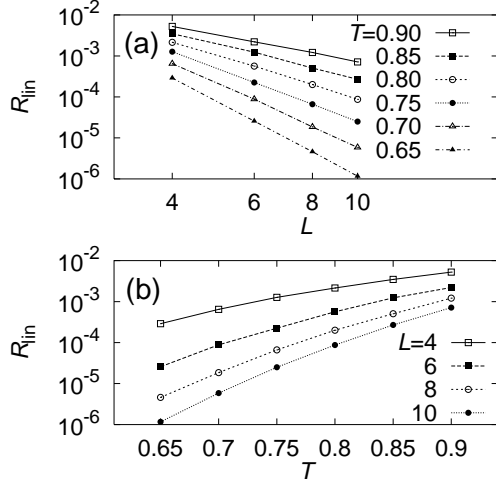


FIG. 1. The linear resistance  $R_{\text{lin}}$  calculated at the trial angle range  $\delta\theta = \pi/6$  in the absence of external current (a) vs system size  $L$  and (b) vs temperature  $T$ . In (a), the dynamic critical exponent  $z$  defined as  $R_{\text{lin}} \sim L^{-z}$  is shown to increase as  $T$  is decreased (see Fig. 2 for  $z$  at various  $\delta\theta$ ).

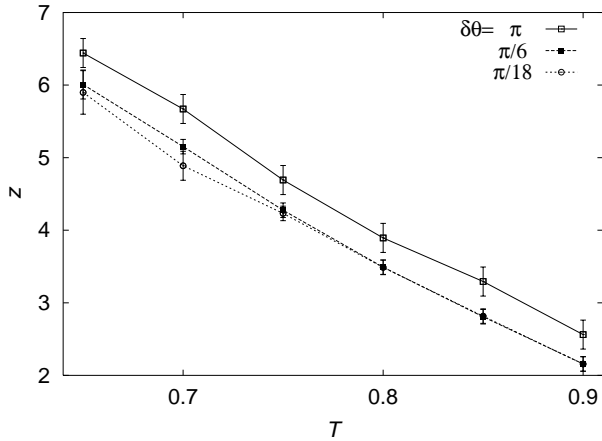


FIG. 2. The dynamic critical exponent  $z$  from the linear resistance  $R_{\text{lin}}$  for the trial angle range  $\delta\theta = \pi$ ,  $\pi/6$ , and  $\pi/18$  (from top to bottom). As  $\delta\theta$  is decreased,  $z$  is shown to saturate and  $z(\delta\theta = \pi/6)$  coincides well with  $z(\delta\theta = \pi/18)$ .

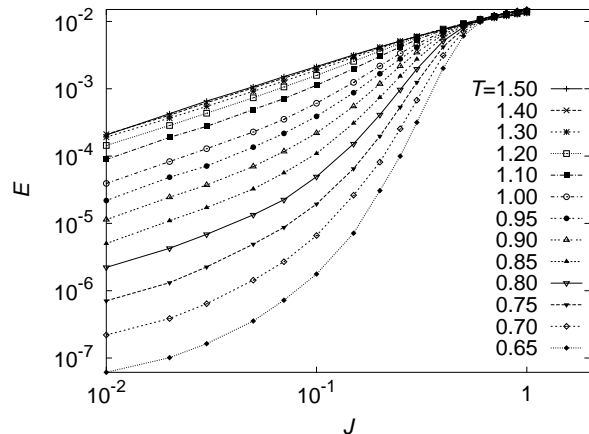


FIG. 3. Current-voltage characteristics (electric field  $E$  vs current density  $J$ ) for  $L = 8$  and the trial angle range  $\delta\theta = \pi/6$  at various temperatures. As  $J$  is decreased the current-voltage characteristics become Ohmic ( $E \propto J$ ) due to finite-size effects.

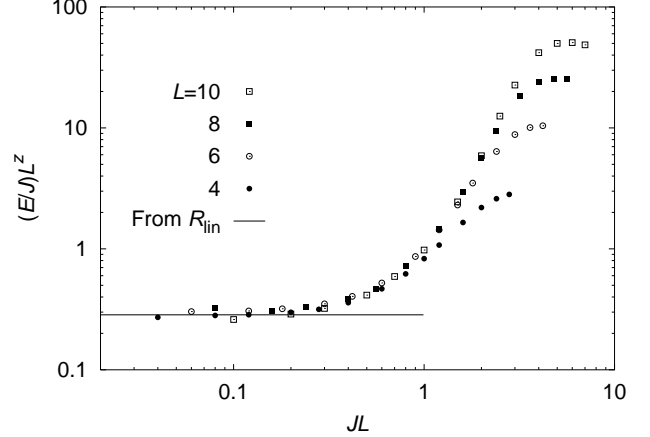


FIG. 4. Finite-size scaling of the current-voltage characteristics,  $(E/J)L^z$  vs  $JL$ , at  $T = 0.80$  and  $\delta\theta = \pi/6$ . The dynamic critical exponent  $z$ , the only one free parameter in the scaling plot, is found to  $z = 3.5(1)$  at  $T = 0.80$ , in agreement with the value in Fig. 2 obtained in the absence of external driving. The horizontal full line denotes  $R_{\text{lin}}L^z$  with  $z = 3.5$  obtained in the absence of an external current, confirming that the simulation results with and without external currents are fully consistent to each other.

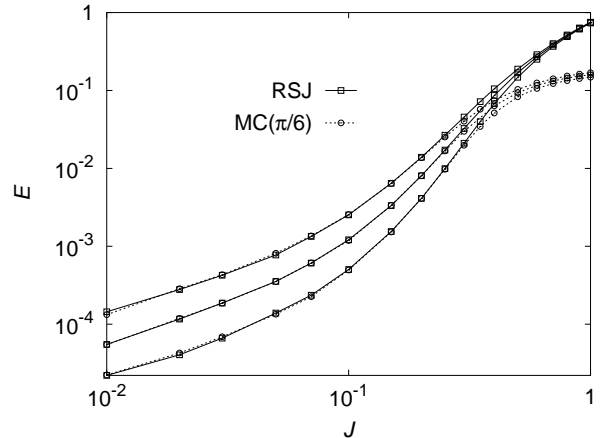


FIG. 5. Comparison of the current-voltage characteristics ( $E$ - $J$ ) of the MC simulation (from Fig. 3) and the RSJ dynamics (in Ref. 19) for  $L = 8$  at  $T = 0.90, 0.85$ , and  $0.80$  (from top to bottom): Multiplications by factors 11.6, 10.9, and 10.1 for  $T = 0.90, 0.85$ , and  $0.80$ , respectively, to  $E$  from MC simulations make two curves coincide very well in a broad range of external current density.